


JES

JOURNAL OF
ENVIRONMENTAL
SCIENCES

ISSN 1001-6742
CN 11-2629/X

March 1, 2014 Volume 26 Number 3
www.jesc.ac.cn

Unexpected malformations in
Xenopus tropicalis



Sponsored by
Research Center for Eco-Environmental Sciences
Chinese Academy of Sciences

CONTENTS

Aquatic environment

- Metal composition of layered double hydroxides (LDHs) regulating ClO_4^- adsorption to calcined LDHs via the memory effect and hydrogen bonding
Yajie Lin, Qile Fang, Baoliang Chen 493
- Limitation of spatial distribution of ammonia-oxidizing microorganisms in the Haihe River, China, by heavy metals
Chao Wang, Baoqing Shan, Hong Zhang, Yu Zhao 502
- Temperature sensitivity of organic compound destruction in SCWO process
Yaqin Tan, Zheming Shen, Weimin Guo, Chuang Ouyang, Jinping Jia, Weili Jiang, Haiyun Zhou 512
- Influence of moderate pre-oxidation treatment on the physical, chemical and phosphate adsorption properties of iron-containing activated carbon
Zhengfang Wang, Mo Shi, Jihua Li, Zheng Zheng 519
- Reduction of DOM fractions and their trihalomethane formation potential in surface river water by in-line coagulation with ceramic membrane filtration
Pharkphum Rakruam, Suraphong Wattanachira 529
- N_2O emission from nitrogen removal via nitrite in oxic-anoxic granular sludge sequencing batch reactor
Hong Liang, Jiaoling Yang, Dawen Gao 537
- Influence of stabilizers on the antimicrobial properties of silver nanoparticles introduced into natural water
Aleksandra Burkowska-But, Grzegorz Sionkowski, Maciej Walczak 542
- Addition of hydrogen peroxide for the simultaneous control of bromate and odor during advanced drinking water treatment using ozone
Yongjing Wang, Jianwei Yu, Dong Zhang, Min Yang 550
- Nitric oxide removal by wastewater bacteria in a biotrickling filter
Hejingying Niu, Dennis Y C Leung, Chifang Wong, Tong Zhang, Mayngor Chan, Fred C C Leung 555
- Elucidating the removal mechanism of *N,N*-dimethyldithiocarbamate in an anaerobic-anoxic-oxic activated sludge system
Yongmei Li, Xianzhong Cao, Lin Wang 566
- Influencing factors of disinfection byproducts formation during chloramination of Cyclops metabolite solutions
Xingbin Sun, Lei Sun, Ying Lu, Jing Zhang, Kejing Wang 575

Atmospheric environment

- Sources of nitrous and nitric oxides in paddy soils: Nitrification and denitrification
Ting Lan, Yong Han, Marco Roelcke, Rolf Nieder, Zucong Cai 581
- Upper Yellow River air concentrations of organochlorine pesticides estimated from tree bark, and their relationship with socioeconomic indices
Chang He, Jun Jin, Bailin Xiang, Ying Wang, Zhaohui Ma 593
- Mechanism and kinetic properties of NO_3 -initiated atmospheric degradation of DDT
Cai Liu, Shanqing Li, Rui Gao, Juan Dang, Wenxing Wang, Qingzhu Zhang 601
- Sorption and phase distribution of ethanol and butanol blended gasoline vapours in the vadose zone after release
Ejike Ugwoha, John M. Andresen 608

Terrestrial environment

- Effects of temperature change and tree species composition on N_2O and NO emissions in acidic forest soils of subtropical China
Yi Cheng, Jing Wang, Shenqiang Wang, Zucong Cai, Lei Wang 617

Environmental biology

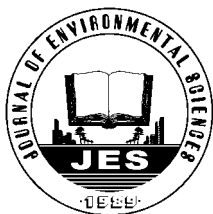
- Influence of sunlight on the proliferation of cyanobacterial blooms and its potential applications in Lake Taihu, China
Qichao Zhou, Wei Chen, Kun Shan, Lingling Zheng, Lirong Song 626
- Bioavailability and tissue distribution of Dechloranes in wild frogs (*Rana limnocharis*) from an e-waste recycling area in Southeast China
Long Li, Wenyue Wang, Quanxia Lv, Yujie Ben, Xinghong Li 636

Environmental health and toxicology

- Unexpected phenotypes of malformations induced in *Xenopus tropicalis* embryos by combined exposure to triphenyltin and 9-*cis*-retinoic acid
Jingmin Zhu, Lin Yu, Lijiao Wu, Lingling Hu, Huahong Shi 643
- Expression of sulfur uptake assimilation-related genes in response to cadmium, bensulfuron-methyl and their co-contamination in rice roots
Jian Zhou, Zegang Wang, Zhiwei Huang, Chao Lu, Zhuo Han, Jianfeng Zhang, Huimin Jiang, Cailin Ge, Juncheng Yang 650

Environmental catalysis and materials

Reaction mechanism and metal ion transformation in photocatalytic ozonation of phenol and oxalic acid with Ag^+/TiO_2 Yingying Chen, Yongbing Xie, Jun Yang, Hongbin Cao, Yi Zhang	662
Effect of TiO_2 calcination temperature on the photocatalytic oxidation of gaseous NH_3 Hongmin Wu, Jinzhu Ma, Changbin Zhang, Hong He	673
Effects of synthesis methods on the performance of Pt + Rh/ $\text{Ce}_{0.6}\text{Zr}_{0.4}\text{O}_2$ three-way catalysts Zongcheng Zhan, Liyun Song, Xiaojun Liu, Jiao Jiao, Jinzhou Li, Hong He	683
Catalytic combustion of soot over ceria-zinc mixed oxides catalysts supported onto cordierite Leandro Fontanetti Nascimento, Renata Figueredo Martins, Rodrigo Ferreira Silva, Osvaldo Antonio Serra	694
Effects of metal and acidic sites on the reaction by-products of butyl acetate oxidation over palladium-based catalysts Lin Yue, Chi He, Zhengping Hao, Shunbing Wang, Hailin Wang	702
Mechanism of enhanced removal of quinonic intermediates during electrochemical oxidation of Orange II under ultraviolet irradiation Fazhan Li, Guoting Li, Xiwang Zhang	708
Serial parameter: CN 11-2629/X*1989*m*223*en*P*26*2014-3	

Available online at www.sciencedirect.com

Journal of Environmental Sciences

www.jesc.ac.cn

Influence of moderate pre-oxidation treatment on the physical, chemical and phosphate adsorption properties of iron-containing activated carbon

Zhengfang Wang, Mo Shi, Jihua Li, Zheng Zheng*

Environmental Science and Engineering Department, Fudan University, Shanghai 200433, China

ARTICLE INFO

Article history:

Received 03 April 2013

revised 14 May 2013

accepted 15 May 2013

Keywords:

adsorption

per-oxidation

iron-containing activated carbon

phosphate

mechanism

DOI: 10.1016/S1001-0742(13)60440-4

ABSTRACT

A novel adsorbent based on iron oxide dispersed over activated carbon (AC) were prepared, and used for phosphate removal from aqueous solutions. The influence of pre-oxidation treatment on the physical, chemical and phosphate adsorption properties of iron-containing AC were determined. Two series of ACs, non-oxidized and oxidized carbon modified by iron (denoted as AC-Fe and AC/O-Fe), resulted in a maximum impregnated iron of 4.03% and 7.56%, respectively. AC/O-Fe showed 34.0%–46.6% higher phosphate removal efficiency than the AC-Fe did. This was first attributed to the moderate pre-oxidation of raw AC by nitric acid, achieved by dosing Fe(II) after a pre-oxidation, to obtain higher iron loading, which is favorable for phosphate adsorption. Additionally, the *in-situ* formed active site on the surface of carbon, which was derived from the oxidation of Fe(II) by nitric acid dominated the remarkably high efficiency with respect to the removal of phosphate. The activation energy for adsorption was calculated to be 10.53 and 18.88 kJ/mol for AC-Fe and AC/O-Fe, respectively. The results showed that the surface mass transfer and intra-particle diffusion were simultaneously occurring during the process and contribute to the adsorption mechanism.

Introduction

With its well-established consequence to eutrophication, the excessive phosphate in wastewater has become an important issue in wastewater treatment (Smith et al., 1999). To limit such pollution, the Chinese Environmental Protection Agency has revised the maximum contaminant level of phosphate in wastewater discharge from 1.0 to 0.5 mg/L according to Class A of Integrated Wastewater Discharge Standard (GB 18918-2002). This new regulatory pressure has increased interest in the development of new or improved technologies to meet the regulation.

Several methods have been developed to remove phosphate from wastewater, namely biological removal and physico-chemical process (Morse et al., 1998). Biological methods could achieve a higher removal rate of phosphate, but the methods are often prone to operational difficulties

and need monitoring. The conventional physico-chemical process used for phosphate removal can be classified on the basis of the involved separation mechanisms: precipitation, membrane, and adsorption technologies. Precipitation with lime, alum, and iron salts has been widely used because of its simplicity and reduced cost; however, in order to remove efficiently phosphate at acceptable levels, large amount of chemicals are necessary. The membrane processes is expensive, mainly because of the high energy requirements. The technology of adsorption is based on materials having high affinity for phosphate. Recently, adsorption of phosphate by metal-based materials has been reported (Zhang et al., 2011a; Zhou et al., 2011).

Activated carbon (AC) has been proven to be an effective adsorbent for the removal of a wide variety of organic and inorganic pollutants from aqueous. However, phosphate adsorption onto raw AC is minimal, it cannot be directly applied for phosphate treatment. Research on AC modification is gaining prominence due to the need to develop

* Corresponding author. E-mail: zzhenghj@fudan.edu.cn.

the affinity of AC for phosphate to facilitate their removal from water. Several publications have shown that the adsorption performance of AC can be evidently improved by treatment with various iron compounds (Muñiz et al., 2009; Fierro et al., 2009), which could be assigned to the fact that iron compounds are cross-linked to AC leading in an enhanced adsorption. It is essential to understand the factors that influence the adsorption of AC prior to their modification to tailor their specific physical and chemical properties and enhance their affinity for phosphate present in wastewaters. Pre-oxidation, using oxidants such as potassium permanganate, hydrogen peroxide, sulfuric and nitric acid, has been shown to enhance the adsorption of pollutants by altering their surface characteristics and charge (Hristovski et al., 2009).

Although several studies have been conducted on pollutants removal (such as arsenic) by iron-containing adsorbents, limited reports address the influence of pre-oxidation treatment on the physical, chemical and phosphate adsorption properties of iron-containing AC. This study aimed to: (1) characterize the modified AC, including nitrogen adsorption analyses, X-ray diffraction (XRD), infrared spectroscopy (FT-IR), and pH_{PZC} analysis; (2) compare the removal efficiencies of phosphate by the modified AC obtained under various preparation conditions; (3) evaluate phosphate adsorption results through both kinetic and equilibrium studies taking into account the major factors including the initial phosphate concentration and temperature; (4) propose the possible reaction mechanism involved in the removal of phosphate by modified AC.

1 Materials and methods

1.1 Preparation of activated carbon

Raw AC sample was supplied by the Masamori Nanjing Chemical Industrial Co., Ltd. (China). The raw AC was thoroughly rinsed with deionized water to remove dust and soluble material and was then allowed to dry at room temperature. Afterwards, the dried sample was modified with 5 mol/L HNO_3 for 6 hr at the room temperature. Oxidized carbon was thoroughly washed by deionized water to remove residual acid adsorbed before iron loading. The carbon oxidized by HNO_3 was named AC/O hereinafter.

The iron-containing AC was prepared by introducing 0.5 g of non-oxidized and oxidized carbon into 100 mL of 0.2 mol/L iron solution made from FeSO_4 . A series of iron concentration ranging from 0.05 to 0.4 mol/L were used for AC coating to examine the effect of iron concentration on phosphate removal. The pH during iron loading ranged from 1.0 to 6.0. The mixtures were stirred continuously for a few minutes, and then heated at 110°C until they become dry. Afterwards, they were cooled at room temperature, rinsed to remove iron residues, dried, and sieved. The

two prepared ACs are denoted as AC-Fe and AC/O-Fe, respectively.

1.2 Characterization of activated carbon

The specific surface area and the porosity of the iron-containing ACs were determined by N_2 adsorption at 77 K using a Micromeritics ASAP-2020 Surface Analyzer in the relative pressure range of 0.01–1. Prior to measurement, all samples were degassed at 120°C and until a constant low pressure was reached ($0.004 \mu\text{mHg}$). The Brunauer-Emmett-Teller (BET) surface areas were calculated using the BET method; micropore volume and micropore specific surface area were obtained using the t-plots method; mesopore volume and mesopore specific surface area were determined by the Barrett-Joyner-Halenda model. The total pore volume was determined by nitrogen uptake at P/P_0 0.98.

XRD measurements were conducted using standard powder diffraction procedure. Mineralogy of the AC samples were analyzed by $\text{Cu K}\alpha$ radiation (40 kV, 30 mA) over the 2θ range 10 – 80° using XRD analysis instrument (ARL, X'TRA, Switzerland).

The functional groups available on the surface of the prepared ACs were identified by KBr technique using a Fourier transform spectrophotometer (Nicolet, Nexus 870 FT-IR, USA). The spectra were recorded from 4000 to 400 cm^{-1} .

Batch equilibrium method was used for determination of the point of zero charge (pH_{PZC}). Accordingly, 0.1 g of the ACs were shaken in PVC vials for 24 hr with 20 mL of 0.01 mol/L KNO_3 , at different pH values. Initial pH values were obtained by adding an amount of KOH or HNO_3 solution (0.01 mol/L), keeping the ionic strength constant. The amount of H^+ or OH^- ions adsorbed by ACs was calculated from the difference between the initial and the final concentration of H^+ or OH^- ions.

1.3 Adsorption experiments

Adsorption experiments were conducted by varying contact time, temperature, initial phosphate concentration under the aspects of adsorption isotherms and adsorption kinetics. Phosphate solutions of 50 mL with different initial concentrations (9.03–39.22 mg/L) were mixed with 0.1 g of AC sample under various temperature (20, 30 and 40°C). The mixture was agitated in a thermostated shaker (Model THZ-C, China) at a speed of 160 r/min at room temperature for 24 hr to reach equilibrium. At predetermined time, the flasks were withdrawn from the shaker and the residual phosphate concentration in the reaction mixture was analyzed by centrifuging the reaction mixture and then measuring the absorbance of the supernatant at 700 nm wave length that correspond to the maximum absorbance of the sample. Phosphate concentration in the reaction mixture was calculated from the calibration curve. All the experiments were performed in duplicates.

The amount of phosphate adsorbed onto AC samples, q_e (mg/g), was calculated by the following mass balance relationship:

$$q_e = (C_0 - C_e)V/W \quad (1)$$

where, C_0 (mg/L) and C_e (mg/L) are the initial and equilibrium concentrations of phosphate solution, respectively; V (L) is the solution volume; and W (g) is the mass of the adsorbent.

The kinetic studies were performed following similar procedure at 20, 30 and 40°C, respectively. The initial concentration was set as 20 mg/L (in P), and the samples were separated at predetermined time intervals. The residual phosphate concentration was analyzed by the same method described above. Each experiment was performed twice under identical conditions.

1.4 Chemical analysis

To test the iron loading on the iron-containing ACs, 0.5 g of samples was ashed at 600°C and then digested with 25 mL of concentrated hydrochloric acid. The digestion solutions were analyzed for iron by atomic absorption spectrophotometer (Hitachi, Z-5000, Japan) with flame atomization.

2 Results and discussion

2.1 Optimization of preparation conditions of activated carbon

Bench-scale tests were done to optimize the preparation conditions of iron-containing AC. The type of iron salt, iron concentration and impregnating pH were considered as crucial factors. The previous studies suggested that the type of iron salt was an important factor that determines the phosphate adsorption efficiency (Wang et al., 2012). The carbon modified by FeSO_4 showed much higher phosphate removal than that modified by FeCl_3 . This is probably because, compared to Fe(II) , Fe(III) easily hydrolyzes to form large metal particle clusters which cannot diffuse easily into the internal pores of AC but are more likely to precipitate in the macropores and coat the outer surfaces of the particles. So the better FeSO_4 modification result might be caused by the fact that better intra-particle diffusion in carbons modified by FeSO_4 which is favored for phosphate adsorption. In this work, AC samples modified by FeSO_4 were tested for removal of phosphate in aqueous solution. Comparative experiments were performed for different preparation conditions, in which the iron concentration varied from 0.05 to 0.4 mg/L, and the impregnating pH varied from 1.0 to 6.0.

The impregnated amounts of iron onto AC were strongly dependent on the impregnating pH (Fig. 1). It could be shown below that the use of very acid solutions (pH =

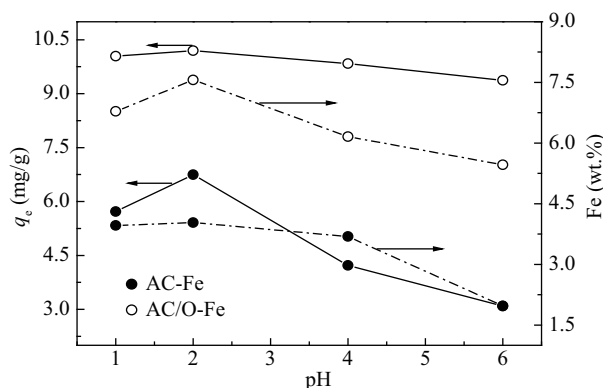


Fig. 1 pH effect on impregnation efficiency of AC-Fe and AC/O-Fe.

1.0) of FeSO_4 was claimed to be ineffective, because the strong affinity of protons for the surface sites would hinder the adsorption of iron (Gu et al., 2005). Both the iron content and the adsorption capacity of modified ACs reached maximum when the impregnating pH was 2.0. And then, gradually reduced impregnation efficiency was noted above pH 2.0, which could be explained by the diffusion efficiency of soluble iron into the pore of AC. Impregnation efficiency of iron on AC could be depend on the diffusion of iron in bulk solution to the meso- or micropores of AC, oxidation of iron to iron oxides and adherence of iron oxides on the AC. The solution pH can greatly affect the diffusion efficiency of iron in bulk solution to the pores of AC because the solubility of iron depends on the solution pH. The impregnation efficiency decreased as the solution pH increased, suggesting the lack of soluble iron which can diffuse into pore of AC (Yang et al., 2009).

The iron content of the raw AC was < 0.05% of Fe per dry carbon weight. Higher iron contents were generally obtained using the pre-oxidation method; these AC/O-Fe samples had 5.46%–7.56% Fe per dry adsorbent weight. The AC-Fe obtained by contacting the carbon with only 0.2 mol/L $\text{FeSO}_4 \cdot 7\text{H}_2\text{O}$ (no pre-oxidation treatment) had a relatively low iron content, 1.97%–4.03% Fe per dry carbon weight. At fixed pH of 2.0, the effects of iron at four concentration levels (0.05, 0.1, 0.2, and 0.4 mol/L) showed that the iron loading on the carbon increased as the iron concentration increased. In general, the phosphate adsorption capacity of both AC-Fe and AC/O-Fe increased as the iron content of the adsorbent increased. However, the iron content did not significantly increase at iron solution concentrations higher than 0.2 mol/L. Furthermore, the increasing iron concentrations did not seem to have a significant effect on the phosphate adsorption capacity of iron-containing ACs. The trend could be explained by the decrease of the high energy adsorption sites due to the excessive iron coating caused a reduction in removal efficiency (Hristovski et al., 2009; Zhang et al., 2008).

The above analysis results thus demonstrated that the pre-oxidation step in this synthesis method is essential to obtain good iron loading, which is favorable for phosphate

adsorption. Based on the above results, appropriate parameters for the preparation conditions were established as: FeSO_4 , impregnating concentrations of 0.2 mol/L Fe and pH of 2.0. The samples prepared under this condition were employed as the iron-containing ACs for further studies, unless otherwise stated.

2.2 Characterization of the activated carbons

2.2.1 Surface area and porosity

The N_2 adsorption/desorption isotherm (Fig. 2) shows that the overall adsorption/desorption curves are comparable between raw AC and modified samples; thus, the basic carbon structures must be maintained during the modified treatment. According to the classification of IUPAC, all the N_2 adsorption/desorption isotherms are considered to be a typical type IV isotherm with a sharp capillary condensation step at high relative pressures ($P/P_0 = 0.85\text{--}0.96$) (Liu et al., 2010). The shape of the hysteresis loop is of a type H4, indicating that raw material and modified samples are predominantly mesoporous, reinforcing the isotherm data (Table 1). The textural properties showed high surface area for all activated carbon samples with a slight reduction after iron impregnation. This effect was more pronounced for the AC/O-Fe, which could be attribute to higher iron content. As the iron contents were increased to 7.56% for AC/O-Fe and 4.03% for AC-Fe, the BET surface areas

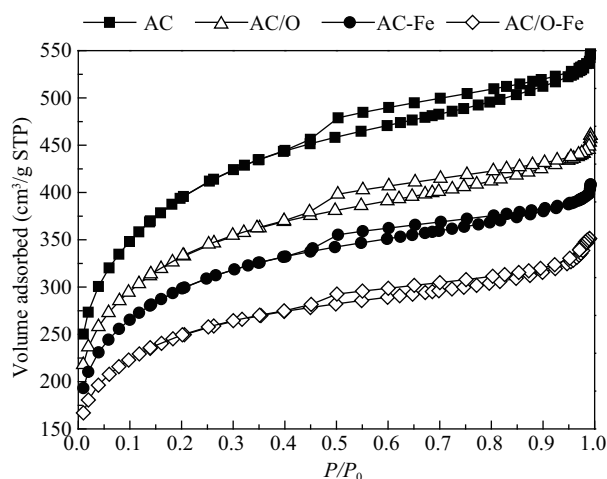


Fig. 2 Adsorption and desorption isotherms of N_2 /77 K. Adsorbed is given in gas volumes at standard temperature and pressure (STP) per gram of adsorbent. STP means $T = 298\text{ K}$, $P = 1\text{ atm}$.

were decreased from 1176.58 to 880.65 m^2/g and from 1406.10 to 1059.67 m^2/g , respectively. It appears that with more iron impregnated, an increasing fraction of pores in the AC is blocked, leading to a lower specific surface area (Castro et al., 2009). The decrease of the mesopore region of AC-Fe and AC/O-Fe might attribute to the blockage of macropores and mesopores by iron metal particles. The corresponding decreases in the total pore volume of AC/O-Fe ranged from 0.71 to 0.54 cm^3/g , the micropore volume from 0.18 to 0.15 cm^3/g , and the mesopore volume from 0.42 to 0.31 cm^3/g .

However, drop of specific surface area and pore volume after modification did not reduce the phosphate adsorption capacity of AC, indicating that physisorption was minor importance for the phosphate uptake. The pre-oxidation treatment before iron loading of raw AC could improve the phosphate adsorption capacity although it slightly decreased the surface area and microporous volume of the samples.

2.2.2 X-ray diffraction analysis

XRD analysis of the raw AC (Fig. 3) showed broad reflection of typically amorphous materials with no appearance of crystallites. The peak at $2\theta = 23.5^\circ$ corresponds to the micrographitic structure characteristic of AC (Castro et al., 2009). The XRD of the modified AC shows new broad bands related to the formed iron phase (Asaoka and Yamamoto, 2010). These new peaks were identified from comparisons with known standards (JCPDS, 2002). The major peaks of AC/O-Fe XRD spectra showed the high intensity and broad peaks of iron in the form of the crystalline iron species goethite ($\alpha\text{-FeOOH}$); while, the XRD spectrum of AC-Fe with the same iron species but relatively low intensity peaks implies a low iron content. In addition, effects of the impregnating pH on the formed iron phase of the iron-containing activated carbon samples obtained by the pre-oxidation treatment were considered. Little difference could be observed between the XRD patterns of AC/O-Fe (pH = 2) and AC/O-Fe (pH = 6). The results indicated that the pre-oxidation treatment shows larger influence on the formation of iron oxide phase than impregnating pH.

2.2.3 FT-IR analysis

The FT-IR spectrums of AC samples are shown in Fig. 4. The FT-IR spectra of AC and AC/O illustrated that there

Table 1 Surface area and porosity parameters of activated carbons

	Surface area (m^2/g)			Pore volume (cm^3/g)			Average pore size (nm)
	BET	Micropore	Mesopore	Micropore	Mesopore	Total	
AC	1406.10	428.07	611.82	0.18	0.51	0.85	2.40
AC/O	1176.58	419.49	471.89	0.18	0.42	0.71	2.42
AC-Fe	1059.67	374.29	424.21	0.16	0.37	0.63	2.39
AC/O-Fe	880.65	351.57	322.60	0.15	0.31	0.54	2.47

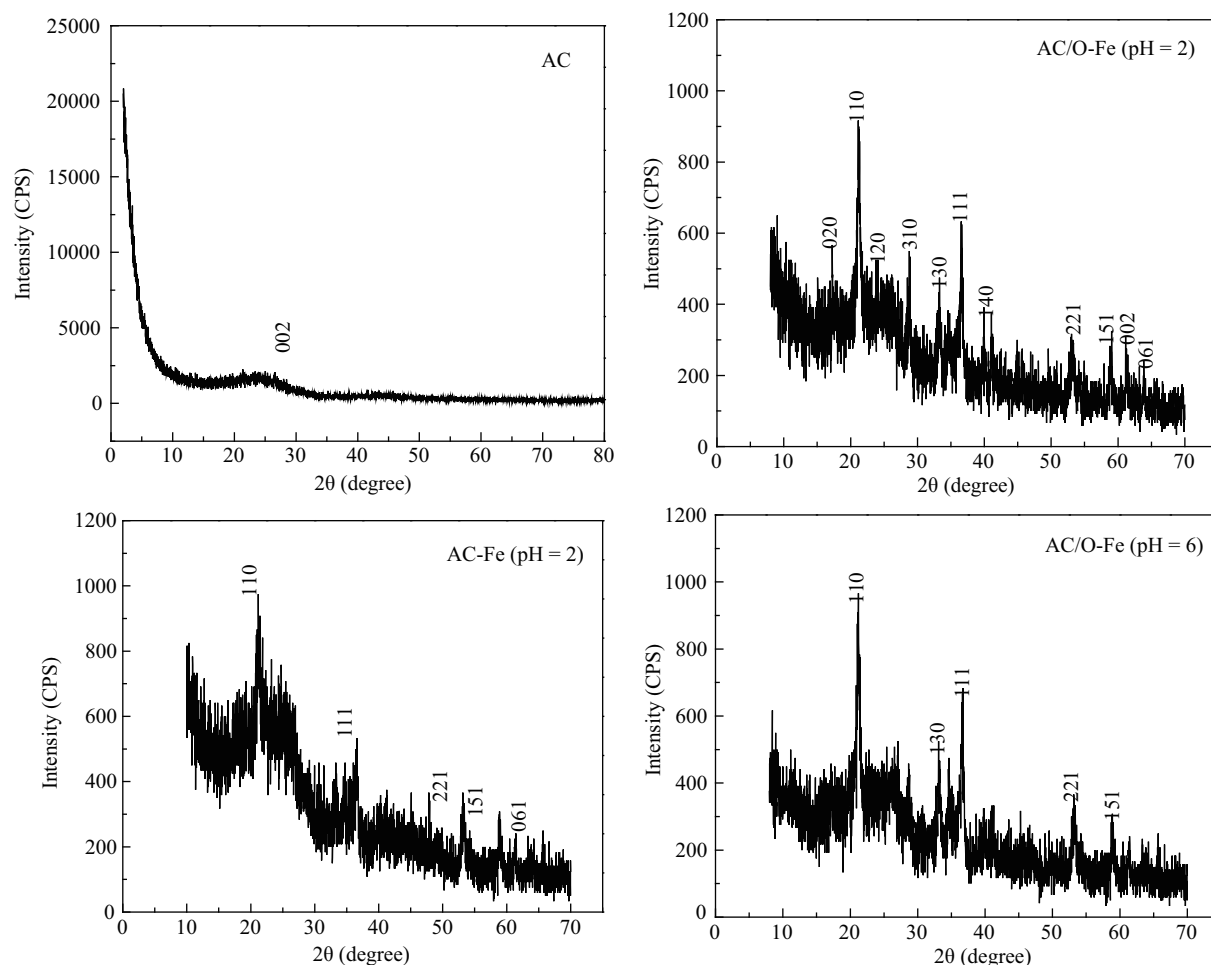


Fig. 3 X-ray diffraction spectra of AC, AC/O-Fe (pH = 2), AC-Fe and AC/O-Fe (pH = 6).

are slightly changes of characteristic bands between 1720 to 1280 cm^{-1} , including the C=O stretching vibration in ketones, aldehydes, lactones and carboxyl groups (1712 cm^{-1}), the C–O stretching in carboxylic groups, and carboxylate moieties (1587 cm^{-1}), and the breathing C–O vibrations in ethers, phenols and hydroxyl groups (1300 cm^{-1}) (Guo and Rockstraw, 2006). Representing oxygen groups, the intensity of these bands was much higher for the oxidized sample (AC/O) than for the AC sample. All of these FT-IR results showed that the pre-oxidation increases some oxygen groups and promotes the crosslinking of AC, and hence, lead to an enhanced equilibrium quantity of fixed iron (Muñiz et al., 2009).

The results of FT-IR phase analysis of the iron-containing activated carbon (AC-Fe and AC/O-Fe) showed a good agreement with those obtained by XRD. The bands between 900 and 795 cm^{-1} can be assigned to Fe–O–H bending vibrations in α -FeOOH (Musić et al., 2003, 2004). The bands between 700 and 400 cm^{-1} were due to the Fe–O stretching vibration (Krishnan and Haridas, 2008). The peaks due to iron-containing functional groups were much more visible for AC/O-Fe than for AC-Fe, indicating the high content of the iron phase in the former

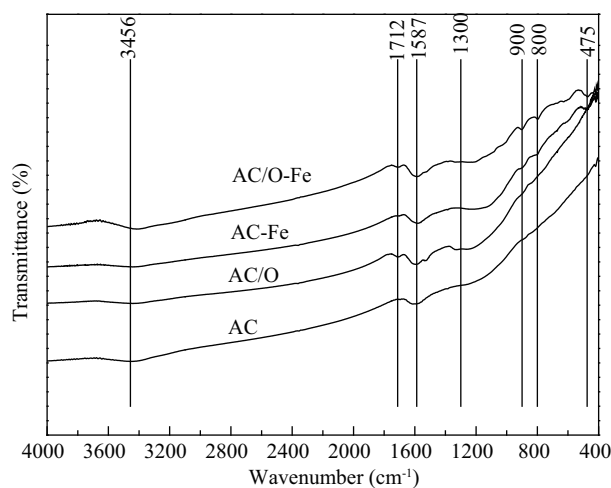


Fig. 4 FT-IR analysis for activated carbon samples.

sample. These observations suggested that the iron was immobilized onto the AC samples by chemical bonding. For the pre-oxidation treatment samples (AC/O-Fe), dissolved ferrous iron diffuses into the internal pores of AC, and followed by oxidation of ferrous to ferric iron. Then the ferric species could cross-link with various oxygen

functional groups on the AC, with a higher content of the iron (Gu et al., 2005).

2.2.4 Surface charge

Experimental results of the pH_{PZC} determination were given as pH values of filtered solutions after equilibration with iron-containing AC as a function of initial pH values of solution. The pH_{PZC} of AC/O-Fe was lower than that of AC-Fe, which was 5.76 for AC/O-Fe and 6.90 for AC-Fe. Pre-oxidation made the materials become more acidic, since the pH_{PZC} systematically decreased. Such a trend is unequivocally correlated to the oxygen content, as already shown by Muñiz et al. (2009). The higher the oxygen level, the higher the acidic character of the AC. This observation for the AC/O-Fe was in general agreement with the trends shown by the FT-IR data (Fig. 2). A negatively charged surface repels more negative phosphate ions; however, positively charged surface attracts more phosphate ions.

2.3 Adsorption results

2.3.1 Adsorption isotherms

The adsorption isotherm plays an important role in the determination of the maximum capacity of adsorption. It suggests how efficiently adsorbent will adsorb and supplies estimate of the economic viability of the adsorbent commercial applications for the solute. In order to adapt for the considered system, an adequate model that can reproduce the experimental results obtained, equations of Langmuir, Freundlich and Redlich-Peterson have been considered.

The validity of the Langmuir model suggests the adsorption process is monolayer and adsorption of each molecule has equal activation energy. As shown in Table 2, for Langmuir isotherm, the values of q_m for both AC-Fe and AC/O-Fe were found to increase with temperature. It suggested that phosphate adsorption onto AC was an endothermic process. Due to the sufficient energy provided by the temperature, more phosphate adsorbed onto AC interior structure. Compared with AC-Fe, the phosphate adsorption capacity of AC/O-Fe was much higher. At 30°C, q_m was calculated to be 7.46 and 13.12 mg/g for AC-Fe and AC/O-Fe, respectively. It suggested that for the sample AC/O-Fe, there were more high energy adsorption sites that lead to strong adsorption (Xiong and Mahmood,

2010). For Freundlich isotherm applies to adsorption on heterogeneous surfaces with interaction between adsorbed molecules, the values of $1/n$ between 0.21 and 0.42 ($0 < 1/n < 1$) indicated the favorability of adsorption of phosphate onto both AC-Fe and AC/O-Fe. Higher K_F values of AC/O-Fe mean higher adsorption/distribution coefficient than that of AC-Fe (Kumar et al., 2010). From the comparisons of the R^2 values for both AC-Fe and AC/O-Fe, the Langmuir isotherm was found to fit the data significantly better than either the Redlich-Peterson or Freundlich isotherm at all temperatures, which shows the more homogeneous nature of the iron-containing activated carbons.

Additionally, we compared maximum adsorption capacities obtained in this study with some other iron-modified activated carbons. Type of activated carbon (Table 3), oxidant used in the pre-oxidation treatment, and preparation methods were considered. The results are listed in Table 4. It was suggested that AC/O-Fe obtained in this research was an effective adsorbent for the purification of wastewater containing phosphate.

2.3.2 Adsorption kinetics

In order to examine the controlling mechanism of adsorption processes such as mass transfer and chemical reaction, pseudo first-order, pseudo second-order and intra-particle diffusion kinetic equations were used to test the experimental data. The pseudo first-order kinetic model suggested by Onganer and Temur (1998) for the adsorption of solid/liquid systems was used to the present study of phosphate adsorption. The rate constant, k_1 and correlation coefficients of phosphate under different temperatures are listed in Table 5. The correlation coefficients for the pseudo first-order kinetic model were low. Moreover, a large difference of equilibrium adsorption capacity (q_e) between the experiment and calculation was observed, indicating a poor pseudo first-order fit to the experimental data.

The kinetic data were further analyzed by pseudo second-order kinetics model (Ho and McKay, 1999). At all studied temperatures, the extremely high correlation coefficients ($R^2 > 0.99$) were obtained. In addition, the calculated q_e values also agreed with the experimental data in the case of pseudo second-order kinetics. It suggested

Table 2 Langmuir, Freundlich, Redlich-Peterson parameters of adsorption isotherms of phosphate onto AC-Fe and AC/O-Fe

Adsorbent	Temperature (°C)	Langmuir			Freundlich			Redlich-Peterson			
		q_m	K_L	R^2	K_F	$1/n$	R^2	α_R	β_R	K_R	R^2
AC-Fe	20	6.59	0.29	0.9719	2.85	0.22	0.9001	0.06	1.54	1.90	0.9640
	30	7.46	0.25	0.9530	3.11	0.22	0.8782	0.56	0.72	1.83	0.9478
	40	8.47	0.25	0.9338	3.69	0.21	0.8364	0.72	0.64	2.15	0.9544
AC/O-Fe	20	9.98	0.49	0.9983	3.76	0.32	0.9150	0.56	0.95	4.88	0.9982
	30	13.12	0.62	0.9939	4.98	0.37	0.8339	0.83	0.85	8.18	0.9681
	40	15.87	0.59	0.9963	5.72	0.42	0.9032	0.69	0.91	9.35	0.9917

Table 3 Main technical specifications of ACs used in the experiment

	Powdered activated carbon	Granular activated carbon	Activated carbon fiber
BET surface areas (m ² /g)	1250–1400	950–1200	1150–1250
Iodine value (mg/g)	1000–1300	≥ 1000	1100–1200
Methylene Blue value (mg/g)	≥ 200	≥ 170	180
Ash content (%)	6–8	6–9	–
Intensity (%)	–	≥ 95%	–
Pore volume (cm ³ /g)	0.8–1.0	0.6–0.9	0.8–1.2
Average pore size (nm)	2.0–3.5	2.0–3.0	1.7–2.0
pH	5–7	5–7	5–7

Table 4 Adsorption capacities for phosphate using iron-modified ACs by different methods

	Oxidant	Preparation method	Adsorption capacity (mg/g)
Powdered activated carbon	HNO ₃	Precipitation ^a	3.248
		Co-impregnation ^b	5.051
		Iron-salt evaporation ^d	13.12
	H ₂ SO ₄	Precipitation ^a	0.835
		Co-impregnation ^b	4.367
		Iron-salt evaporation ^c	6.249
Granular activated carbon	HNO ₃	Precipitation ^a	1.358
		Co-impregnation ^b	1.450
		Iron-salt evaporation ^c	2.104
	H ₂ SO ₄	Precipitation ^a	0.573
		Co-impregnation ^b	1.384
		Iron-salt evaporation ^c	2.016
Activated carbon fiber	HNO ₃	Precipitation ^a	2.492
		Co-impregnation ^b	4.360
		Iron-salt evaporation ^c	4.967
	H ₂ SO ₄	Precipitation ^a	0.937
		Co-impregnation ^b	1.143
		Iron-salt evaporation ^c	3.286

The data were adopted from ^a Thirunavukkarasu et al. (2003); ^b Fierro et al. (2009); ^c Vaishya and Gupta (2003); and ^d this study.

Table 5 Adsorption kinetic parameters of phosphate onto AC-Fe and AC/O-Fe

Adsorbent	Temperature (°C)	q_{exp} (mg/g)	Pseudo first-order			Pseudo second-order			Intra-particle diffusion		
			q_e (mg/g)	k_1 (min ⁻¹)	R^2	q_e (mg/g)	k_2 (g/(mg·min))	R^2	k_p (mg/(g·min ^{0.5}))	C (mg/g)	R^2
AC-Fe	20	6.72	4.23	0.0254	0.9888	6.99	0.0127	0.9969	0.5512	1.82	0.9914
	30	7.23	4.62	0.0266	0.9876	7.41	0.0164	0.9979	0.3883	3.49	0.9261
	40	7.94	4.89	0.0260	0.9901	8.12	0.0166	0.9979	0.4384	3.82	0.9952
AC/O-Fe	20	9.97	5.27	0.0317	0.9312	10.22	0.0120	0.9974	0.6670	3.91	0.8944
	30	10.07	7.47	0.0324	0.9700	10.24	0.0167	0.9980	0.3820	6.20	0.9657
	40	10.58	8.23	0.0422	0.9177	10.70	0.0197	0.9986	0.3852	6.93	0.9978

that the adsorption data are well represented by pseudo second-order kinetics and this supports the assumption (Ho and McKay, 1999) that the rate-limiting step of phosphate onto iron-containing AC may be chemisorption. From **Table 5**, the values of the rate constant k_2 increased with increasing temperature. It was explained that as temperature increased, the surface activity and kinetic energy of adsorbent also increased which caused the interaction forces between the solute and adsorbent to become stronger.

2.3.3 Intra-particle diffusion study

In order to gain insight into the mechanism of adsorption process and to determine the rate controlling step which is mainly depends on either surface or pore diffusion, Weber's intra-particle diffusion model was adopted (Weber and Morris, 1963). This model is expressed as follows:

$$q_t = k_p t^{0.5} + C \quad (2)$$

where, C (mg/g) is the intercept and k_p (mg/(g·min^{0.5})) is the intra-particle diffusion rate constant, which can be

evaluated from the slope of the linear plot of q_t versus $t^{0.5}$. If the regression of q_t versus $t^{0.5}$ is linear and passes through the origin, then intra-particle diffusion is the sole rate-limiting step (Weber and Morris, 1963). However, it was observed that the intra-particle diffusion model of phosphate adsorption on AC-Fe and AC/O-Fe were both not linear over the whole time range and the plots obtained presented multi-linearity (not shown here). The linear plots did not pass through the origin and this deviation from the origin might be due to the difference in mass transfer rate in the initial and final stages of adsorption. From these results, it could be concluded that intra-particle diffusion is not the dominating mechanism for the adsorption of phosphate on both AC-Fe and AC/O-Fe (Ahmed and Theydan, 2012). The intra-particle diffusion rate constant (k_p) and C are reported in **Table 5**. The C value reflects the boundary layer effect (Weber and Morris, 1963). The C values increased with the temperature, which indicated an increase of the thickness of the boundary layer and therefore internal mass transfer is favored over surface mass transfer (El Nemr et al., 2008). Taking into account the effects of time, it was proposed that intra-particle diffusion plays an important role in the adsorption. Larger C values of AC/O-Fe than that of AC-Fe might mean better intra-particle diffusion in AC/O-Fe which is favored for phosphate adsorption.

2.3.4 Surface mass transfer study

The uptake of phosphate from liquid phase (sorbate) to solid surface (adsorbent) is carried out by transfer of mass from the former to the latter. The phosphate adsorption process by AC-Fe and AC/O-Fe can both be divided into three phases. The first step was the mass transfer of sorbate from the aqueous phase on to the solid surface. The second step was the sorption of solute on to the surface sites of the adsorbent. And the last step was the internal diffusion of solute via either a pore diffusion model or homogeneous solid phase diffusion model.

During the present study, the second step has been assumed rapid enough with respect to the other steps and therefore it is not rate limiting in any kinetic study. Taking into account these probable steps, mass transfer analysis for the removal of phosphate was carried out using kinetic model proposed by McKay et al. (1981) which describes the transfer of adsorbate in solution; with the assumption the adsorption obeys the Langmuir model. This model is expressed as follows:

$$\ln\left(\frac{C_t}{C_0} - \frac{1}{1+mK_L}\right) = \ln\left(\frac{mK_L}{1+mK_L} - \frac{1+mK_L}{mK_L}\beta_L S_0 t\right) \quad (3)$$

where, C_t (mg/L) is the concentration after time t , C_0 (mg/L) is the initial concentration, m (g/L) is the mass of adsorbent per unit volume of particle-free absorbate solution, K_L (L/g) is the constant obtained by Langmuir equation, and β_L (cm/sec) the mass transfer coefficient. S_0 (cm⁻¹) is the outer surface of adsorbent per unit volume of

particle-free solution, given as:

$$S_0 = \frac{6m}{D_a d(1-\epsilon)} \quad (4)$$

where, D_a (cm) is the diameter, d (g/cm³) is the density and ϵ is the porosity of the adsorbent.

As shown in **Fig. 5**, plot of $\ln(C_t/C_0 - 1/(1+mK_L))$ versus t for phosphate gives the straight line. The linear nature of the plot confirms the validity of the diffusion model for the phosphate-carbon system (Daifullah et al., 2007). For AC-Fe, the values of β_L (3.10×10^{-7} , 3.40×10^{-7} and 3.70×10^{-7} cm/min) were calculated from the slopes and intercepts of the plots (**Fig. 5**) of $\ln(C_t/C_0 - 1/(1+mK_L))$ versus t (min) at different temperatures (20, 30 and 40°C). The values of β_L obtained for AC/O-Fe (1.52×10^{-6} , 2.40×10^{-6} and 4.10×10^{-6} cm/min) showed that the rate of transfer of mass from bulk solution to the adsorbent surface was rapid enough so it cannot be rate controlling step (Gupta et al., 1988). Larger β_L values of AC/O-Fe than that of AC-Fe might mean better surface mass transfer in AC/O-Fe which is favored for phosphate adsorption. It could also be mentioned that the deviation of some points from the linearity of the plots suggested the varying extent of mass transfer at the initial and final stages of the adsorption (Hasan et al., 2008).

2.3.5 Activation energy

Arrhenius equation is expressed as follows,

$$k = k_0 \exp\left(\frac{-E_a}{RT}\right) \quad (5)$$

$$\ln(k) = \ln(k_0) - \frac{E_a}{R}\left(\frac{1}{T}\right) \quad (6)$$

where, k (g/(mg·min)) is the rate constant of pseudo-second order adsorption, k_0 is the Arrhenius factor, R (8.314 J/(mol·K)) is gas constant, T (K) is absolute temperature. The activation energy (E_a) can be calculated from

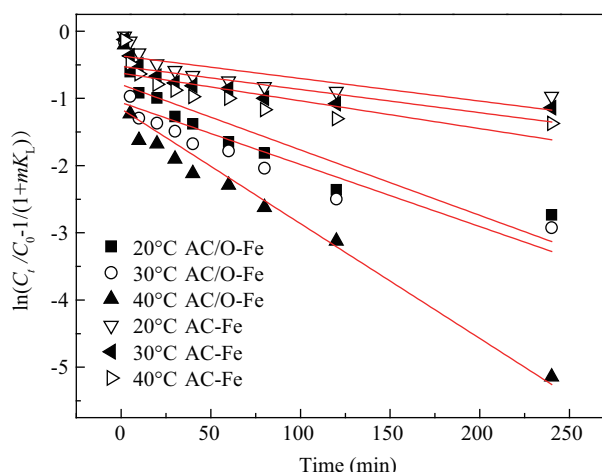


Fig. 5 Mass transfer plot for the adsorption of phosphate on iron-containing activated carbons at different temperatures.

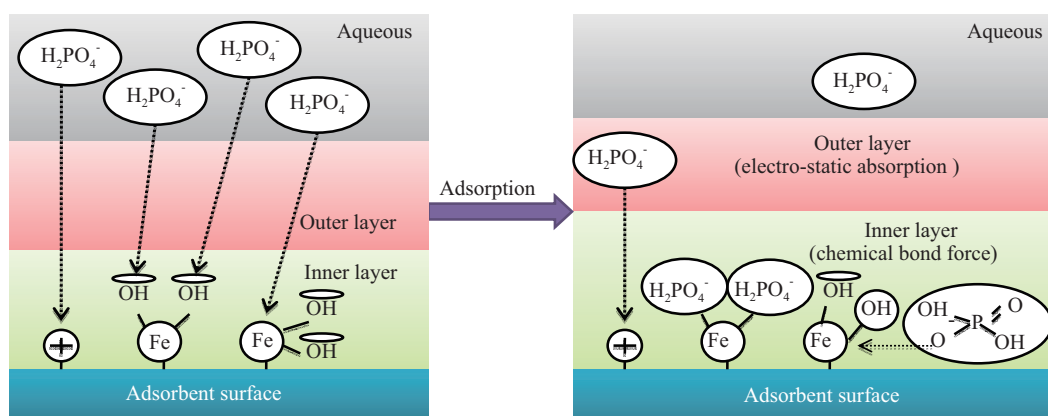


Fig. 6 Proposed mechanism of phosphate uptake on iron-containing activated carbon.

Arrhenius equation, which is useful for estimating the type of adsorption process. Due to the weak forces between the adsorbent and adsorbate, E_a value for physical adsorption is usually lower than 4.2 kJ/mol. Chemical adsorption involves forces much stronger than physical adsorption. The adsorption process could be assigned to chemical adsorption if E_a values are between 8.4 and 83.7 kJ/mol (Smith, 1981). In this study, E_a value for adsorption were found to be 10.53 and 18.88 kJ/mol for AC-Fe and AC/O-Fe, respectively, both falling in the chemical adsorption range. Compared to AC-Fe, the activation energy of AC/O-Fe was more higher, which is related to better adsorption capacity. This result for the AC/O-Fe was strongly consistent with the above analysis.

2.3.6 Proposed adsorption mechanism

After the pre-oxidation and iron-doped treatment, the activated carbon became more chemically stable, and provided more activate and accessible sites to adsorb phosphate molecules (Fig. 6). From kinetic and isotherm analysis, and high activation energy of the iron-containing activated carbons, we could assume that the phosphate-carbon reaction could be dominated by a chemical adsorption mechanism through electro-static adsorption in the outer layer and chemical bond force in the inner layer (Tian et al., 2009; Zhang et al., 2011b). AC/O-Fe has a higher phosphate removal capacity than AC-Fe, which could be attributed to its higher affinity toward phosphate probably due to the existence of the above-mentioned interactions. The adsorption process was complex; both chemical adsorption, surface mass transfer and intra-particle diffusion were simultaneously occurring during the process and contribute to the adsorption mechanism.

3 Conclusions

This study has demonstrated that the iron-containing adsorbent for phosphate was successfully prepared by

loading iron onto the surface of activated carbon, which was confirmed based on the results of XRD and FT-IR. Both the adsorption performance and kinetics indicated that modification process by pre-oxidation treatment is a promising approach for enhancement of the phosphate adsorption capacity. The equilibrium adsorption data agreed reasonably well for Langmuir isotherm model. Adsorption dynamic study revealed that the adsorption process followed pseudo second-order equation. The AC/O-Fe gave more percentage removal of phosphate than that of AC-Fe, which could be attributed to its better surface mass transfer, intra-particle diffusion and higher binding energy. Due to its high efficiency for phosphate treatment, easy commercial availability, and working experience of water treatment, the iron-containing activated carbon can be considered a useful adsorbent for phosphate.

Acknowledgments

This study was supported by the Major Science and Technology Program for Water Pollution Control and Treatment (No. 2012ZX07102-004).

REFERENCES

- Ahmed, M.J., Theydan, S.K., 2012. Equilibrium isotherms, kinetics and thermodynamics studies of phenolic compounds adsorption on palm-tree fruit stones. *Ecotoxicol. Environ. Saf.* 84, 39–45.
- Asaoka, S., Yamamoto, T., 2010. Characteristics of phosphate adsorption onto granulated coal ash in seawater. *Mar. Pollut. Bull.* 60(8), 1188–1192.
- Castro, C.S., Guerreiro, M.C., Oliveira, L.C.A., Goncalves, M., Anastacio, A.S., Nazzarro, M., 2009. Iron oxide dispersed over activated carbon: Support influence on the oxidation of the model molecule methylene blue. *Appl. Catal. A* 367(1–2), 53–58.
- Daifullah, A.A.M., Yakout, S.M., Elreedy, S.A., 2007. Adsorption of fluoride in aqueous solutions using KMnO_4 -modified activated carbon derived from steam pyrolysis of rice straw. *J. Hazard. Mater.* 147(1–2), 633–643.
- El Nemr, A., Khaled, A., Abdelwahab, O., El-Sikaily, A., 2008. Treatment of wastewater containing toxic chromium using new activated

- carbon developed from date palm seed. *J. Hazard. Mater.* 152(1), 263–275.
- Fierro, V., Muniz, G., Gonzalez-Sanchez, G., Ballinas, M.L., Celzard, A., 2009. Arsenic removal by iron-doped activated carbons prepared by ferric chloride forced hydrolysis. *J. Hazard. Mater.* 168(1), 430–437.
- Gu, Z.M., Fang, J., Deng, B.L., 2005. Preparation and evaluation of GAC-based iron-containing adsorbents for arsenic removal. *Environ. Sci. Technol.* 39(10), 3833–3843.
- Guo, Y.P., Rockstraw, D.A., 2006. Physical and chemical properties of carbons synthesized from xylan, cellulose, and kraft lignin by H_3PO_4 activation. *Carbon* 44(8), 1464–1475.
- Gupta, G.S., Prasad, G., Singh, V.N., 1988. Removal of colour from wastewater by sorption for water reuse. *J. Environ. Sci. Health* 23, 205–218.
- Hasan, S.H., Singh, K.K., Prakash, O., Talat, M., Ho, Y.S., 2008. Removal of Cr(VI) from aqueous solutions using agricultural waste 'maize bran'. *J. Hazard. Mater.* 152(1), 356–365.
- Ho, Y.S., McKay, G., 1999. Pseudo-second order model for sorption processes. *Process Biochem.* 34(5), 451–465.
- Hristovski, K.D., Westerhoff, P.K., Moller, T., Sylvester, P., 2009. Effect of synthesis conditions on nano-iron (hydr)oxide impregnated granulated activated carbon. *Chem. Eng. J.* 146(2), 237–243.
- Krishnan, K.A., Haridas, A., 2008. Removal of phosphate from aqueous solutions and sewage using natural and surface modified coir pith. *J. Hazard. Mater.* 152(2), 527–535.
- Kumar, P.S., Ramalingam, S., Senthamarai, C., Niranjana, M., Vijayalakshmi, P., Sivanesan, S., 2010. Adsorption of dye from aqueous solution by cashew nut shell: Studies on equilibrium isotherm, kinetics and thermodynamics of interactions. *Desalination* 261(1–2), 52–60.
- Liu, Y., Li, K.X., Sun, G.H., 2010. Effect of precursor preoxidation on the structure of phenolic resin-based activated carbon spheres. *J. Phys. Chem. Solids* 71(4), 453–456.
- McKay, G., Otterburn, M.S., Sweeney, A.G., 1981. Surface mass-transfer processes during colour removal from effluent using silica. *Water Res.* 15(3), 327–331.
- Morse, G.K., Brett, S.W., Guy, J.A., Lester, J.N., 1998. Review: Phosphorus removal and recovery technologies. *Sci. Total Environ.* 212(1), 69–81.
- Muñiz, G., Fierro, V., Celzard, A., Furdin, G., Gonzalez-Sánchez, G., Ballinas, M.L., 2009. Synthesis, characterization and performance in arsenic removal of iron-doped activated carbons prepared by impregnation with Fe(III) and Fe(II). *J. Hazard. Mater.* 165(1–3), 893–902.
- Musić, S., Krehula, S., Popović, S., 2004. Effect of HCl additions on forced hydrolysis of FeCl_3 solutions. *Mater. Lett.* 58(21), 2640–2645.
- Musić, S., Krehula, S., Popović, S., Skoko, Z., 2003. Some factors influencing forced hydrolysis of FeCl_3 solutions. *Mater. Lett.* 57(5–6), 1096–1102.
- Onganer, Y., Temur, C., 1998. Adsorption dynamics of Fe(III) from aqueous solutions onto activated carbon. *J. Coll. Interface Sci.* 205(2), 241–244.
- Smith, J.M., 1981. *Chemical Engineering Kinetic* (3rd ed.). McGraw-Hill, Singapore, 676.
- Smith, V.H., Tilman, G.D., Nekola, J.C., 1999. Eutrophication: Impacts of excess nutrient inputs on freshwater, marine, and terrestrial ecosystems. *Environ. Pollu.* 100(1–3), 179–196.
- Thirunavukkarasu, O.S., Viraraghavan, T., Subramanian, K.S., 2003. Arsenic removal from drinking water using granular ferric hydroxide. *Water Sa.* 29(2), 161–170.
- Tian, S.L., Jiang, P.X., Ning, P., Su, Y.H., 2009. Enhanced adsorption removal of phosphate from water by mixed lanthanum/aluminum pillared montmorillonite. *Chem. Eng. J.* 151(1–3), 141–148.
- Vaishya, R.C., Gupta, S.K., 2003. Arsenic removal from groundwater by iron impregnated sand. *J. Environ. Eng.* 129(1), 89–92.
- Wang, Z.F., Nie, E., Li, J.H., Yang, M., Zhao, Y.J., Luo, X.Z. et al., 2012. Equilibrium and kinetics of adsorption of phosphate onto iron-doped activated carbon. *Environ. Sci. Poll. Res.* 19(7), 2908–2917.
- Weber, W.J., Morris, J.C., 1963. Kinetics of adsorption on carbon from solution. *J. Sanit. Eng.* 89(2), 31–60.
- Xiong, J.B., Mahmood, Q., 2010. Adsorptive removal of phosphate from aqueous media by peat. *Desalination* 259(1–3), 59–64.
- Yang, J.K., Park, H.J., Lee, H.D., Lee, S.M., 2009. Removal of Cu(II) by activated carbon impregnated with iron(III). *Coll. Surf. A* 337(1–3), 154–158.
- Zhang, J., Shen, Z., Mei, Z., Li, S., Wang, W., 2011a. Removal of phosphate by Fe-coordinated amino-functionalized 3D mesoporous silicates hybrid materials. *J. Environ. Sci.* 23(2), 199–205.
- Zhang, L., Wan, L.H., Chang, N., Liu, J.Y., Duan, C., Zhou, Q. et al., 2011b. Removal of phosphate from water by activated carbon fiber loaded with lanthanum oxide. *J. Hazard. Mater.* 190(1–3), 848–855.
- Zhang, N., Lin, L.S., Gang, D.C., 2008. Adsorptive selenite removal from water using iron-coated GAC adsorbents. *Water Res.* 42(14), 3809–3816.
- Zhou, J.B., Yang, S.L., Yu, J.G., Shu, Z., 2011. Novel hollow microspheres of hierarchical zinc-aluminum layered double hydroxides and their enhanced adsorption capacity for phosphate in water. *J. Hazard. Mater.* 192(3), 1114–1121.



Editorial Board of Journal of Environmental Sciences

Editor-in-Chief

Hongxiao Tang Research Center for Eco-Environmental Sciences, Chinese Academy of Sciences, China

Associate Editors-in-Chief

Jiuhui Qu Research Center for Eco-Environmental Sciences, Chinese Academy of Sciences, China
Shu Tao Peking University, China
Nigel Bell Imperial College London, United Kingdom
Po-Keung Wong The Chinese University of Hong Kong, Hong Kong, China

Editorial Board

Aquatic environment

Baoyu Gao
Shandong University, China
Maohong Fan
University of Wyoming, USA
Chihpin Huang
National Chiao Tung University
Taiwan, China
Ng Wun Jern
Nanyang Environment &
Water Research Institute, Singapore
Clark C. K. Liu
University of Hawaii at Manoa, USA
Hokyoung Shon
University of Technology, Sydney, Australia
Zijian Wang
Research Center for Eco-Environmental Sciences,
Chinese Academy of Sciences, China
Zhiwu Wang
The Ohio State University, USA
Yuxiang Wang
Queen's University, Canada
Min Yang
Research Center for Eco-Environmental Sciences,
Chinese Academy of Sciences, China
Zhifeng Yang
Beijing Normal University, China
Han-Qing Yu
University of Science & Technology of China

Terrestrial environment

Christopher Anderson
Massey University, New Zealand
Zucong Cai
Nanjing Normal University, China
Xinbin Feng
Institute of Geochemistry,
Chinese Academy of Sciences, China
Hongqing Hu
Huazhong Agricultural University, China
Kin-Che Lam
The Chinese University of Hong Kong
Hong Kong, China
Erwin Klumpp
Research Centre Juelich, Agrosphere Institute
Germany
Peijun Li
Institute of Applied Ecology,
Chinese Academy of Sciences, China

Michael Schlöter

German Research Center for Environmental Health
Germany
Xuejun Wang
Peking University, China
Lizhong Zhu
Zhejiang University, China

Atmospheric environment

Jianmin Chen
Fudan University, China
Abdelwahid Mellouki
Centre National de la Recherche Scientifique
France
Yujing Mu
Research Center for Eco-Environmental Sciences,
Chinese Academy of Sciences, China
Min Shao
Peking University, China
James Jay Schauer
University of Wisconsin-Madison, USA
Yuesi Wang
Institute of Atmospheric Physics,
Chinese Academy of Sciences, China
Xin Yang
University of Cambridge, UK

Environmental biology

Yong Cai
Florida International University, USA
Henner Hollert
RWTH Aachen University, Germany
Jae-Seong Lee
Hanyang University, South Korea
Christopher Rensing
University of Copenhagen, Denmark
Bojan Sedmak
National Institute of Biology, Ljubljana
Lirong Song
Institute of Hydrobiology,
the Chinese Academy of Sciences, China
Chunxia Wang
National Natural Science Foundation of China
Gehong Wei
Northwest A & F University, China
Daqiang Yin
Tongji University, China
Zhongtang Yu
The Ohio State University, USA

Environmental toxicology and health

Jingwen Chen
Dalian University of Technology, China
Jianying Hu
Peking University, China
Guibin Jiang
Research Center for Eco-Environmental Sciences,
Chinese Academy of Sciences, China
Sijin Liu
Research Center for Eco-Environmental Sciences,
Chinese Academy of Sciences, China
Tsuyoshi Nakanishi
Gifu Pharmaceutical University, Japan
Willie Peijnenburg
University of Leiden, The Netherlands
Bingsheng Zhou
Institute of Hydrobiology,
Chinese Academy of Sciences, China

Environmental catalysis and materials

Hong He
Research Center for Eco-Environmental Sciences,
Chinese Academy of Sciences, China
Junhua Li
Tsinghua University, China
Wenfeng Shangguan
Shanghai Jiao Tong University, China
Yasutake Teraoka
Kyushu University, Japan
Ralph T. Yang
University of Michigan, USA

Environmental analysis and method

Zongwei Cai
Hong Kong Baptist University,
Hong Kong, China
Jiping Chen
Dalian Institute of Chemical Physics,
Chinese Academy of Sciences, China
Minghui Zheng
Research Center for Eco-Environmental Sciences,
Chinese Academy of Sciences, China

Municipal solid waste and green chemistry

Pinjing He
Tongji University, China
Environmental ecology
Rusong Wang
Research Center for Eco-Environmental Sciences,
Chinese Academy of Sciences, China

Editorial office staff

Managing editor Qingcai Feng
Editors Zixuan Wang Suqin Liu Zhengang Mao
English editor Catherine Rice (USA)

JOURNAL OF ENVIRONMENTAL SCIENCES

环境科学学报(英文版)
(<http://www.jesc.ac.cn>)

Aims and scope

Journal of Environmental Sciences is an international academic journal supervised by Research Center for Eco-Environmental Sciences, Chinese Academy of Sciences. The journal publishes original, peer-reviewed innovative research and valuable findings in environmental sciences. The types of articles published are research article, critical review, rapid communications, and special issues.

The scope of the journal embraces the treatment processes for natural groundwater, municipal, agricultural and industrial water and wastewaters; physical and chemical methods for limitation of pollutants emission into the atmospheric environment; chemical and biological and phytoremediation of contaminated soil; fate and transport of pollutants in environments; toxicological effects of terrorist chemical release on the natural environment and human health; development of environmental catalysts and materials.

For subscription to electronic edition

Elsevier is responsible for subscription of the journal. Please subscribe to the journal via <http://www.elsevier.com/locate/jes>.

For subscription to print edition

China: Please contact the customer service, Science Press, 16 Donghuangchenggen North Street, Beijing 100717, China. Tel: +86-10-64017032; E-mail: journal@mail.sciencep.com, or the local post office throughout China (domestic postcode: 2-580).

Outside China: Please order the journal from the Elsevier Customer Service Department at the Regional Sales Office nearest you.

Submission declaration

Submission of an article implies that the work described has not been published previously (except in the form of an abstract or as part of a published lecture or academic thesis), that it is not under consideration for publication elsewhere. The submission should be approved by all authors and tacitly or explicitly by the responsible authorities where the work was carried out. If the manuscript accepted, it will not be published elsewhere in the same form, in English or in any other language, including electronically without the written consent of the copyright-holder.

Submission declaration

Submission of the work described has not been published previously (except in the form of an abstract or as part of a published lecture or academic thesis), that it is not under consideration for publication elsewhere. The publication should be approved by all authors and tacitly or explicitly by the responsible authorities where the work was carried out. If the manuscript accepted, it will not be published elsewhere in the same form, in English or in any other language, including electronically without the written consent of the copyright-holder.

Editorial

Authors should submit manuscript online at <http://www.jesc.ac.cn>. In case of queries, please contact editorial office, Tel: +86-10-62920553, E-mail: jesc@263.net, jesc@rcees.ac.cn. Instruction to authors is available at <http://www.jesc.ac.cn>.

Journal of Environmental Sciences (Established in 1989)

Vol. 26 No. 3 2014

Supervised by	Chinese Academy of Sciences	Published by	Science Press, Beijing, China
Sponsored by	Research Center for Eco-Environmental Sciences, Chinese Academy of Sciences		Elsevier Limited, The Netherlands
Edited by	Editorial Office of Journal of Environmental Sciences P. O. Box 2871, Beijing 100085, China Tel: 86-10-62920553; http://www.jesc.ac.cn E-mail: jesc@263.net , jesc@rcees.ac.cn	Distributed by	Domestic Science Press, 16 Donghuangchenggen North Street, Beijing 100717, China Local Post Offices through China Foreign Elsevier Limited http://www.elsevier.com/locate/jes
Editor-in-chief	Hongxiao Tang	Printed by	Beijing Beilin Printing House, 100083, China
CN 11-2629/X	Domestic postcode: 2-580		Domestic price per issue RMB ¥ 110.00

ISSN 1001-0742

